Paper ID: FM-08

Numerical Investigation of Aerodynamic and Structural Performance of a Centrifugal Compressor

Roohany Mahmud[1], Rofiques Salehin[2], Wing Commander S A Savanur[3]
[1,2,3]Department of Aeronautical Engineering
Military Institute of Science & Technology (MIST)
Mirpur Cantonment, Dhaka-1216, Bangladesh
E-mail: roohany.mahmud@gmail.com[1], rsalehin92@gmail.com[2], shrinisavy@gmail.com[3]

Abstract

Centrifugal compressors with high pressure ratio are generally used in turbochargers and turboshaft engines because of their small dimensions, high efficiency and wide operating range. By understanding the flow phenomena we can largely improve the performance of a high pressure ratio centrifugal compressor. In this paper, the flow field in a centrifugal compressor of expected pressure ratio of almost 1.83 with a vaneless diffuser has been investigated numerically on the design point. A finite-volume based CFD solver is used in this purpose. Furthermore, the temperature and pressure loads obtained from aerodynamic analysis are used to simulate the structural stresses and deformations on the blade body. This structural performance is assessed with and without the presence of rotational velocity of the addressed centrifugal compressor. Finally, the authors hope that this paper will help the future designers about upgrading aerodynamic performance of a centrifugal compressor within structural limitations in mind before going for the final design and manufacturing.

Keywords: Centrifugal Compressor, Impeller, Tip Speed, Relative Mach number

1. Introduction

Centrifugal compressors are generally designed to transfer energy from a set of rotating impeller blades to the gas. The term "centrifugal" implies that the gas flow is radial, and the energy transfer is caused from a change in the centrifugal forces acting on the gas. Centrifugal compressors deliver high flow capacity per unit of installed space and weight, have good stability, better resistance and less susceptibility to the loss of performance. Moreover, they require significantly less maintenance than axial compressors. Centrifugal compressor are still in used for wide variety of products ranging from small commuter aircraft to large industrial petrochemical compressor stations. To make a low weight and small size centrifugal compressors the designers generally stick with two principles during designing: 1) To increase the compressor's specific speed to reduce the rotor exit diameter and thus to reduce the weight and size in a specific stage, 2) To increase the pressure ratio in a stage to reduce the requirement of number of stages which, in turn, will reduce the machine's weight and size. But this gives rise to a problem, i.e., the increase in Mach number in the flow inside the machine. Centrifugal compressors with transonic Mach number levels often has low efficiencies which may be due to the impact of shocks and shock/boundary layer interactions on rotor and diffuser flow.

The main objective of this paper is to demonstrate a complete computational fluid dynamics (CFD) analysis of a three-dimensional centrifugal compressor within geometric and flow constraints. The study will highlight the different important flow characteristics at different regions of the compressor parts. Finally, a structural effect on the solid body of the impeller due to the generated temperature and pressure load is described.

2. Numerical Aspects

The Navier-Stokes equations for steady-state flow in their conservation form is solved for the computational fluid dynamic analysis. Three transport equations of mass, momentum and energy in conservation form and two constitutive equations of state for density and for enthalpy are summed up to form a closed system. The turbulence model used here is k-epsilon which is used often in industrial applications and has very good convergence behavior. The structural analysis of the impeller is done for a linear isotropic material – structural steel. Finite element method (FEM) is adopted for the static structural analysis of the 3-D impeller system. As the main objective of the paper is show the CFD and structural analysis results, so we will not discuss about the fundamental governing equations and property relations, as they can easily be found in[1,2].

3. Computational model of the centrifugal Compressor

3.1. Case model

For the current analysis, we consider a centrifugal compressor which will operate on average sea-level pressure and temperature (design point). The expected pressure ratio is 1.83 at a mass-flow rate of 0.3 kg/s through the machine rotating at 60000 rpm. Moreover, it is assumed that the compressor has a hub and shroud diameter of 30 mm and 60 mm respectively. The compressor impeller consists of nine main blades and nine splitter blades with backsweep angle of 45^0. For the impeller blade sets, the vane normal thickness at hub and at shroud is assumed 1.8 mm and 0.5 mm respectively. The axial tip clearance is 0.03 mm. From these assumed values, we can calculate the flow coefficient, tip width, flow angles and specific speed by iterative process. Thus, we can create 3-D geometry of the compressor impeller. The splitter blades have the same geometric characteristics like the main blades. The material used for the structural analysis is structural steel. The fluid used here is air ideal gas. From the specified geometric characteristics and the operating conditions the performance curve for the investigated model is determined.

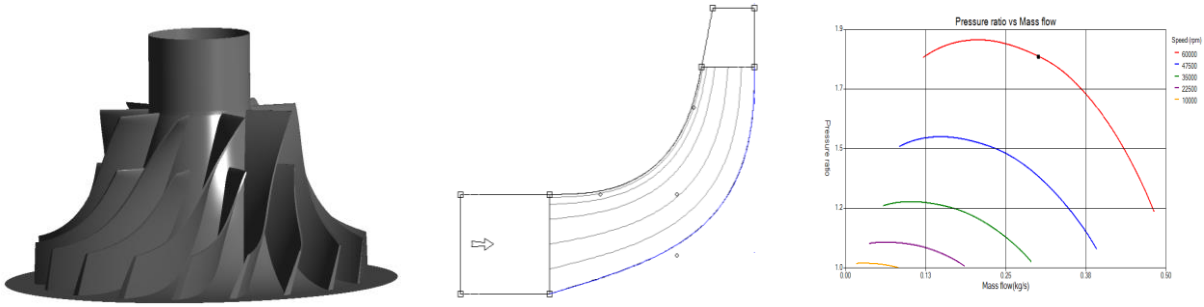

(a) (b) (c)

Fig. 1. (a) 3-D geometry of Compressor, (b) Meridional view of impeller, (c) Performance Curve

3.2. Grid distribution

For the purpose of solving the governing partial differential equations for CFD and structural model the geometry needs to be discretized over which the equations can be approximated. The grid generation for the investigated model has been done separately for two cases: CFD analysis and structural analysis. For the CFD case part, the geometry of the compressor model is discretized with anisotropic hexahedral mesh. A refined layer of mesh is created near the wall boundary and impeller tip region. Along the highly curved surfaces, the 'body-fitted' non-orthogonal structured grids generate which reduces the mesh generation time and also the solution time efficiently. The mesh for structural model is generated using sweeping method from shroud to hub. The generated mesh is hexahedral dominant with some prism layer meshes. The orthogonality factor and skewness are checked for the structural model meshes and are found to be in acceptable range.

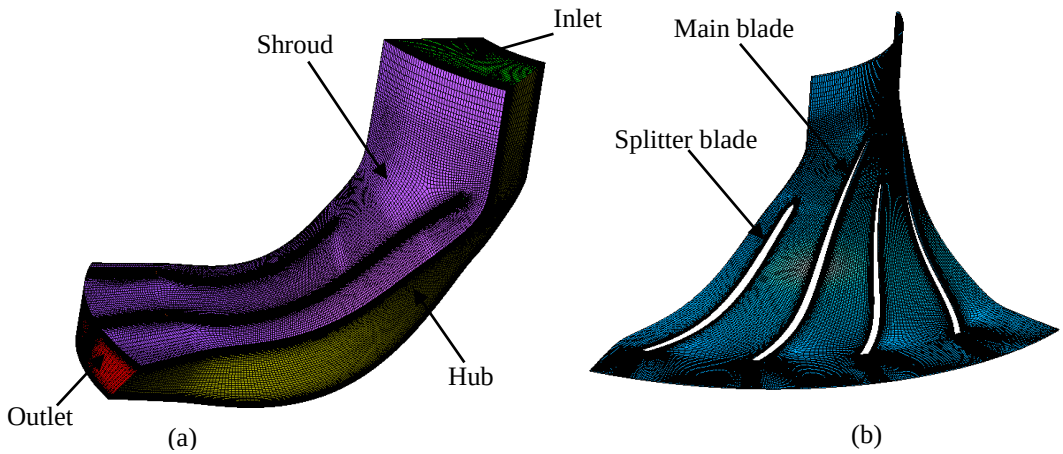

(a) (b)

Fig. 2. (a) 3-D mesh view of an impeller, (b) Mesh elements at 50% of span

3.3. Grid Independency Verification

It is necessary to carry out the independency verification of the grid system before CFD computation. From the performance curve of centrifugal compressor at design flow rate of 0.3 kg/s, with a rotating speed of 60000 rpm, the expected pressure ratio is 1.83. The grid independency test is performed for five grid system. And finally we have chosen the 2 million fine mesh for the CFD problem to better capture the flow near the wall region. The solid blade body has 170177 nodes and 25250 elements for structural analysis.

Table 1. Total Pressure ratio for different grid system (CFD case)

Total Nodes	Total Elements	Total Pressure ratio
401746	370521	1.86
432300	399300	1.87
874680	822898	1.87
1381800	1312002	1.86
1982890	1894220	1.86

3.4. Numerical simulation method

A steady-state turbulent flow simulation method is adopted for the CFD analysis. The rotational axis of the hub is along the negative z-axis of the global coordinate system. The fluid domain consists of inlet, outlet and main passage. A solid domain is created comprising of the main blade and splitter blade, extracted from the fluid domain and meshed separately for the purpose of structural analysis. A fluid-solid interface is existed where the fluid domain touches the solid domain. And, along the tip clearance there also exists fluid-fluid interface. Hub and shroud are in rotating frame of reference and with respect to them inlet and outlet are in stationary frame of reference. For the CFD analysis, a pressure inlet and mass flow outlet is specified. Again, for hub and shroud wall no-slip condition and adiabatic heat transfer option are assigned. Adiabatic heat transfer option is available through the solid blade body. Additionally, for the structural analysis two cases are considered. In one case there is no rotational velocity and for the other case, rotationally induced inertial effect is considered. The face attached to the hub is considered to be as a fixed support. Pressure and temperature loads are imported from the CFD analysis to determine the equivalent stresses and total deformation in the blade body.

4. Results and discussions

4.1. Relative Mach number and velocity distribution

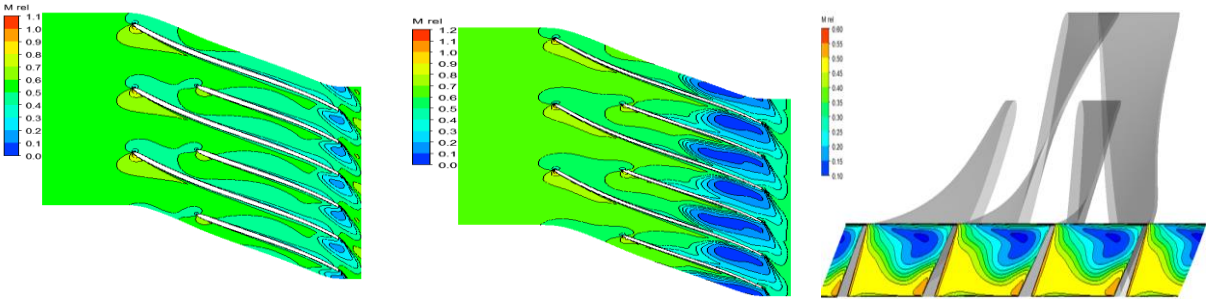

(a) (b) (c)

Fig. 3. Contour of relative Mach number at (a) 50% span, (b) 80% span, (c) blade trailing edge

From fig. 3 it can be seen that the relative Mach number is gradually increasing from leading to trailing edge of the main blade along the streamlines, but due to the presence of splitter blade the flow diffuses and tends to have a similar pattern of flow in the impeller exit. The vane needs to be carefully designed as transonic flow is found to be in the impeller leading edge. In fig. 3(a) and 3(b) small shock waves are seen in the leading edge which may lead to severe instabilities and corresponding losses. Flow separation is apparent near the trailing edges and thickens near the shroud due to the tip clearance effect, and thus causes larger blockage in the flow path. The use of splitter blades largely reduces the wake region and improves the mass flow through the impeller exit. Fig. 4 depicts that the flow is well attached, smooth and homogeneous, except flow reversal is seen near the shroud tip region due to the tip clearance effect. Again, due to the pressure difference between the pressure surface and

suction surface of the impeller, vortex flow generates downstream of the impeller and reduces the velocity of the air at the adjacent streamlines.

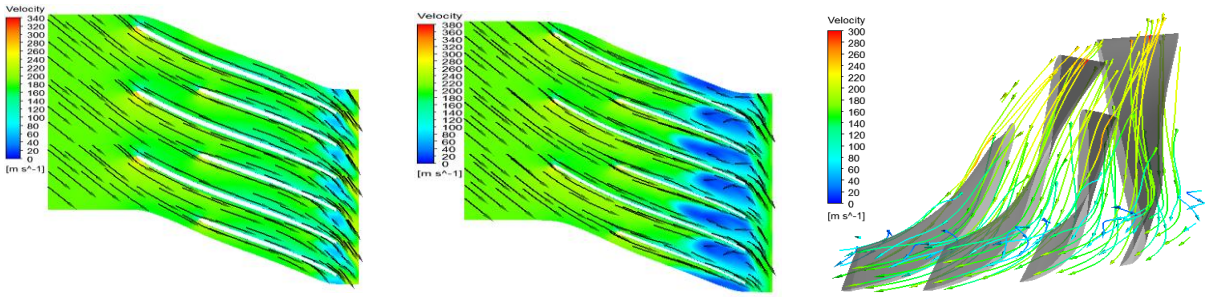

(a) (b) (c)

Fig. 4. Velocity vectors at (a) 50% span, (b) 80% span and (c) Velocity streamlines

4.2. Pressure distribution and entropy change

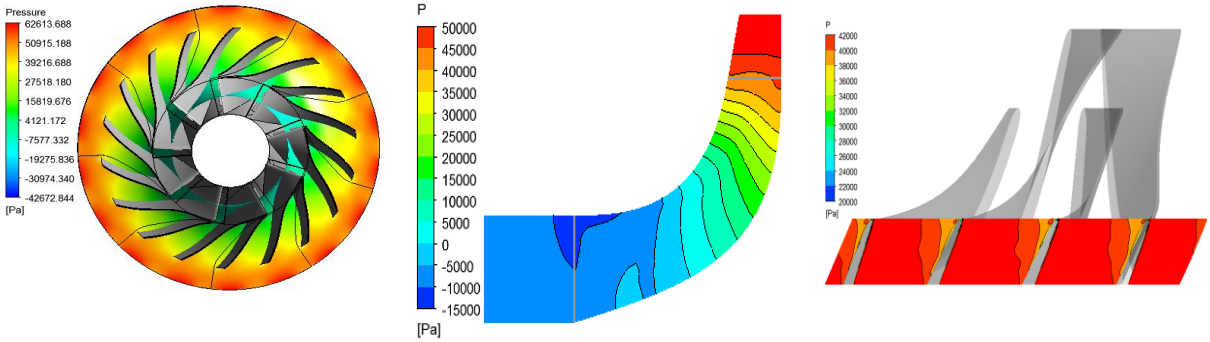

(a) (b) (c)

Fig. 5. (a) Pressure distribution at 50% span, (b) Contour of pressure on Meridional Surface, (c) Contour of Pressure at blade trailing edge

The fig. 5(a) shows the pressure distribution between the blade to blade passage from inlet to outlet in streamwise direction when the centrifugal compressor operating at design conditions. The pressure increases gradually along stream-wise direction and due to the presence of splitter blade the pressure is almost homogeneous on both pressure and suction surfaces. From fig. 5(c), we can observe that, the pressure at impeller exit is very smooth along the throat area except a slight decrease in pressure head near the suction side tip region. Fig. 5(b) shows the smooth increase of meridional surface pressure along the streamwise direction and also the choke flow region near the impeller inlet. As a result, there is a certain decrease in downstream pressure in the impeller inlet region and causes instabilities and vibrations in the machine.

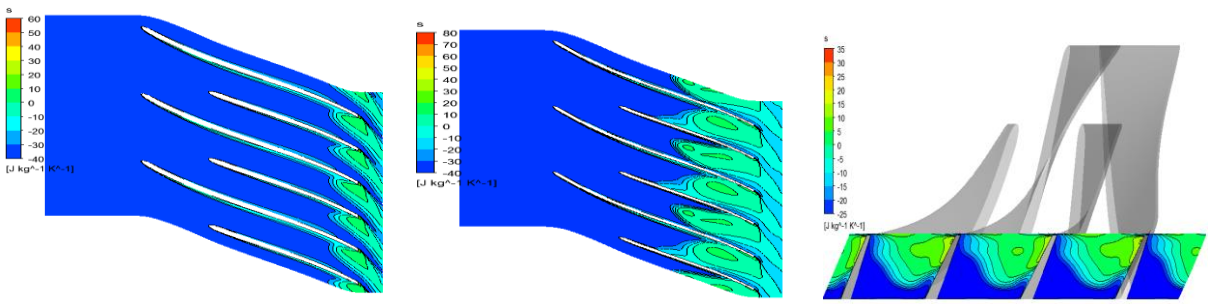

(a) (b) (c)

Fig. 6. Entropy change at (a) 50% span, (b) 80% span and (c) contour of entropy change at blade trailing edge

Fig. 6 points out the entropy change in blade-to-blade passage across streamwise direction and in throat area at blade trailing edge. Entropy at the wall of impeller leading edge is maximum due to the presence of shock wave. Again, entropy close to the blade side wall is higher than the blade passage due to the boundary layer effect. As flow reversal and tip leakage flow are prominent at region near the shroud, higher entropy is observed at impeller exit and even in the blade passage.

4.3. Turbulence kinetic energy and gas compressor performance

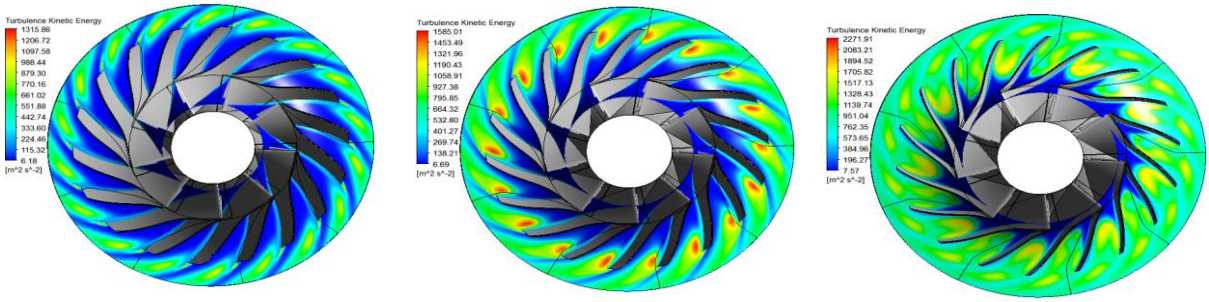

(a) (b) (c)

Fig. 7. Turbulence kinetic energy at (a) 20% span, (b) 50% span and (c) 80% span

Behavior of turbulence in a centrifugal compressor is very difficult to calculate accurately and is not very well known till date. The turbulence model used here is k-epsilon which solves for two variables: k; the turbulent kinetic energy, and epsilon; the rate of dissipation of kinetic energy. Turbulence starts at impeller leading edge and increases far downstream of the flow. The generation of vortex at tip due to the pressure difference between the pressure and suction sides moves in the opposite direction of the compressor rotation, convecting turbulence into the passage**.** Turbulence in the blade passage is more prominent near the shroud region than the hub due to the tip clearance effect. Moreover, the turbulence is higher near the blade wall than the blade passage.
The distribution of other flow parameters such as static and total temperature, pressure and enthalpy along the streamline or span of the blade were also studied. The averaged results tabulated here will be helpful in understanding the overall performance of the compressor.

Table 2. Gas compressor performance

Parameters	Inlet	Outlet	Ratio(Out/In)
Temperature	280.418 K	331.976 K	1.18386409782334
Total Temperature	288.001 K	350.846 K	1.21821205249311
Pressure	92291.2 kg m^-1 s^-2	155618 kg m^-1 s^-2	1.68616474289756
Total Pressure	101321 kg m^-1 s^-2	188938 kg m^-1 s^-2	1.86474778384332
Enthalpy	-17810.3 m^2 s^-2	33975.3 m^2 s^-2	-1.90761612767174
Total Enthalpy	-10194.1 m^2 s^-2	52927.5 m^2 s^-2	-5.19195371732098

4.4. Equivalent stresses

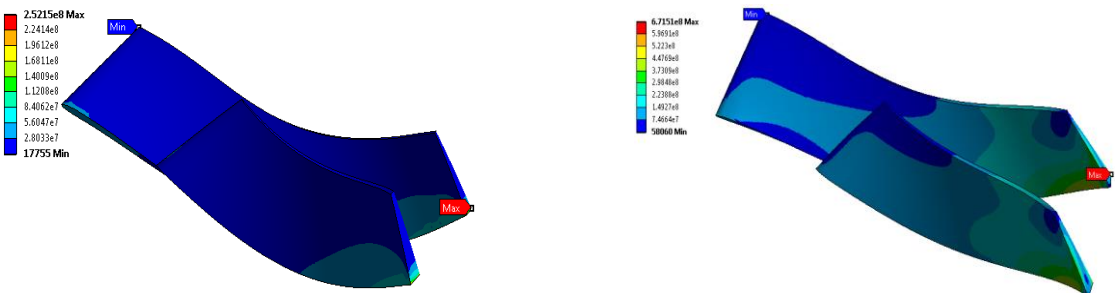

(a) (b)

Fig. 8. Equivalent stress distribution (in Pascal) (a) without rotation (case-1), (b) with rotation (case-2)

The mechanical stress experienced by the impeller set due to the pressure and temperature loading through the machine is shown in fig. 8 for two cases: (a) without rotation and (b) with rotation. The maximum stress in case-2 is much larger than case-1, as there is no rotationally induced inertial effect in case-1. Moreover, the equivalent stress distribution at different span of impeller is much larger in case-2. The maximum stress is found at hub tip region for both cases. It is also evident that the blade thickness from hub to shroud strongly influences the von Mises stress. The initial design was done in such way that the blade thickness increases from shroud to hub to counter the high stress regions. In reference [6] it is shown that the hub blade thickness has little impact on compressor efficiency. For the impeller set, the maximum stress in main blade is slightly higher than the splitter blade. The high stress region near the tip is justified as the pressure, temperature and the rotational velocity all are increasing from leading to trailing edge of the impeller.

4.5. Total deformations

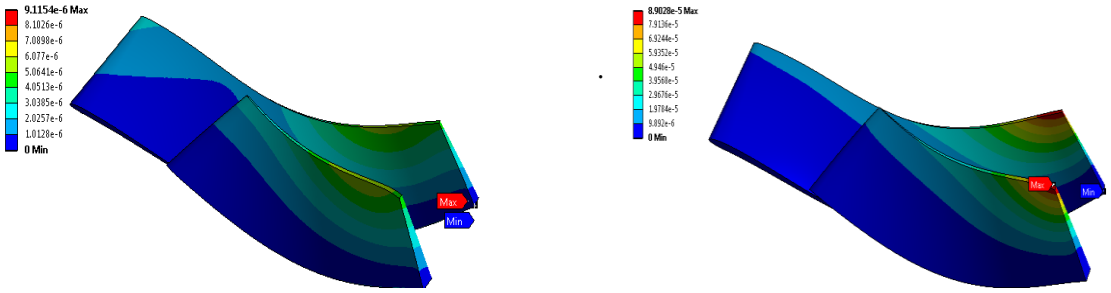

(a) (b)

Fig. 9. Total deformation (in meter) (a) without rotation, (b) with rotation

Another mechanical property evaluated is total deformation of the impeller blade set. It is previously mentioned that the tip clearance between shroud and tip of the main blade is 0.03mm. So, the maximum allowable blade tip deformation must be equal to or lower than this value. For case-1 the maximum value of deformation is 0.009mm which is in allowable range. But, for case-2, due to the rotational velocity the deformation at tip is 0.089mm which is larger than tip clearance gap. So, we need to increase the gap between blade and shroud cover above 0.089mm which in turn, increases the secondary flow and tip leakage and causes further losses.

5. Conclusion

The complex centrifugal compressor internal flow field is investigated by using the k-epsilon turbulence model along with the simulation of 3-D steady Navier–Stokes equations. The internal flow simulation of the centrifugal compressor demonstrates the flow pattern and pressure distribution of the compressor operating at design point. The velocity vector is almost homogeneous on both pressure and suction side surfaces but, tip leakage and flow reversal exist near the impeller exit which is dominant near the shroud tip region. As for pressure distribution, the pressure increases gradually along the streamwise direction and the presence of splitter blade causes a smooth pressure distribution on both side of the blade. Small shock regions are observed near the leading edge which causes loss in energy head. For the structural analysis, the trailing edge tip is found to be the most critical region. Although, convergence and mesh generation all are in acceptable range, a physical experimentation of the addressed centrifugal compressor is still required to justify the numerical values generated during the simulation process. This paper can still help designers in choosing different parameters during the primary design phase.

6. References

[1] H. Versteeg, W. Malalasekera, An Introduction to Computational Fluid Dynamics: The Finite Volume Method, Prentice Hall, 2nd edition, 2007.

[2] Egor P. Popov, Mechanics of Materials, Prentice Hall, 2nd edition, 1976.

[3] S Larry Dixon and Cesare Hall, Fluid Mechanics and Thermodynamics of Turbomachinery, Butterworth-Heinemann, 7thd edition, November 13, 2013.

[4] H. Cohen, GFC Rogers and HIH Saravanamuttoo, Gas Turbine Theory, Longman Group Limited, 4th edition, 1996.

[5] H. David Joslyn, Joost J. Brasz, and Robert P. Dring, "Centrifugal Compressor Impeller Aerodynamics: An Experimental Invesitgation", Journal of Turbomachinery, Vol.113, No.4, pp. 660-669, 1991.

[6] T. Verstraete, Z. Alsalihi, R.A. Van den Braembussche, "Multidisciplinary optimization of a radial compressor for microgas turbine applications", Journal of Turbomachinery, Vol. 132, 2010.